Effects of Continuous Steam Explosion on the Microstructure and Properties of Eucalyptus Fibers

Pengtao Ma, Junshan Lan, Yanhong Feng,* Rongliang Liu, Jinping Qu, and Hezhi He

Laboratory-designed continuous steam explosion (CSE) equipment was used to prepare continuous steam-exploded eucalyptus fibers (CSEEFs). The pretreatment intensity was varied by changing treatment time, and effects of CSE on the composition, microstructure, surface composition, thermal properties, and crystallinity of CSEEFs were investigated. Composition analysis showed that CSE had a significant impact on lignin and hemicellulose, but little on cellulose. Scanning electron microscopy indicated that the middle lamella, primary wall, and outer secondary wall were progressively stripped as the CSE time increased. X-ray photoelectron spectroscopy demonstrated that concentrations of extractives and lignin were higher on the surface of eucalyptus wood than CSEEFs', and the exposed carbohydrate fraction increased with increasing CSE time. Differential scanning calorimetry showed that eucalyptus wood has one glass transition (193.5 °C), whereas two glass transitions at 56.7 and 138.5 °C were observed for CSEEF-5. X-ray diffraction results suggested that crystallinity of samples decreased with increasing CSE time. Thermogravimetric analysis showed the pyrolysis peak temperature of samples first increased and then decreased slightly as CSE time increased. These data will be useful for the optimization and application of CSE technology.

Keywords: Continuous steam explosion; Eucalyptus; Microstructure; Surface composition; Property

*Contact information: National Engineering Research Center of Novel Equipment for Polymer Processing, The Key Laboratory of Polymer Processing Engineering of the Ministry of Education, South China University of Technology, Guangzhou 510641, PR China; *Corresponding author: yhfeng@scut.edu.cn*

INTRODUCTION

Wood fibers are an environmentally friendly and renewable natural resource. Researchers have made substantial progress in exploring ways to efficiently and comprehensively use wood resources. The major components of wood fibers are cellulose, lignin, hemicellulose, and small amounts of extractives. These components contribute to wood fiber properties, which ultimately affect the properties of plants and the products derived from them (Samira *et al.* 2015). Fiber cells are the most basic unit of plant fibers. The walls of fiber cells are composed of cellulose microfibrils and matrix polymers. The layered structure of a typical wood fiber cell is depicted in Fig. 1 (Sjöström 1993). The middle lamella is the layer that holds neighboring cells together. The lignin proportion is higher in the middle lamella than in the primary and secondary walls (Kadla and Gilbert 2000). The middle lamella and the two adjacent primary walls are often referred to as the compound middle lamella. The thicknesses of the middle lamella and primary wall are approximately 0.2 to 1.0 μm and 0.1 to 0.2 μm, respectively. The thicker secondary wall consists of three distinct layers, labeled in Fig. 1 as S1, S2, and S3, from the outer to the inner layer. The S1 and S3 layers are the thinnest, while the S2 layer is the thickest (1 to 5

μm) and primarily responsible for the strength of individual fibers. These layers differ from one another in structure and chemical composition. The microfibrils of the secondary wall wind helically around the fiber axis at different angles depending on the layer, while those of the primary wall are randomly oriented (Wardrop 1963; Salmén and Ljunggren 1996). The angle of microfibrils to the fiber axis can be used to identify which layer the microfibrils belong to.

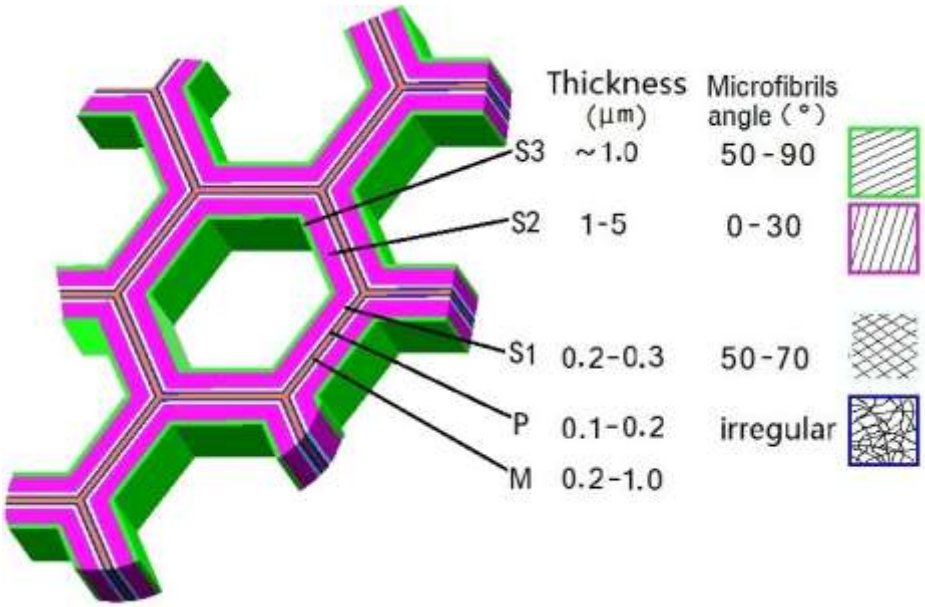

Fig. 1. Structure of a fiber cell and the average thickness and microfibril angle of the middle lamella (M), primary wall (P), and layers of the secondary wall (S1, S2, and S3)

Appropriate pretreatment of plant fibers can significantly increase the efficiency of use of plant biomass for the production of chemicals, biofuels, and degradable biomaterials. One energy-efficient and environmentally friendly pretreatment method is steam explosion (SE). SE is usually carried out in batches: wood chips are placed in a reactor and high-pressure steam is applied for a short period of time. The steam is then rapidly vented from the reactor to reduce pressure, and the contents are discharged into a large vessel to flash-cool the biomass. It has been demonstrated that SE causes both mechanical tearing and chemical degradation (Chen and Liu 2007). The treatment results in substantial disruption of fiber structure, hydrolysis of the hemicellulosic fraction, depolymerization of the lignin components, and defibration of cellulose (Moniruzzaman 1996; Martín-Sampedro *et al*. 2012). Researchers have proposed a multiscale model of biomass pretreatment relating to operation, material, and equipment parameters for the optimization of equipment design and SE conditions (Zhang and Chen 2012). Martín-Sampedro *et al.* (2014) showed that SE was more efficient than steam treatment for delignification of *Eucalyptus globulus* wood. Law *et al.* (1989, 1990) found that fiber separation in SE-treated black spruce (*Picea mariana*) occurred primarily in the middle lamella. Although SE treatment does not significantly increase the biological methane potential of wheat straw during anaerobic digestion, it does increase the degradation rate (Basurto Gutierrez *et al*. 2012; Theuretzbacher *et al*. 2015). This increase occurs because SE at an appropriate intensity removes hemicellulose and lignin and increases the specific surface area, improving the accessibility of cellulose.

The characteristics of plant fibers are influenced by surface composition (Koljonen *et al*. 1997). X-ray photoelectron spectroscopy (XPS) has long been used to assess the surface composition of plant fibers. Gray *et al*. (2010) reviewed XPS methods and presented a simplified approach to estimate surface lignin content. Using XPS, Hua *et al.* (1993a, b) found that there were more carbohydrates on the fiber surface after SE treatment. Negro *et al*. (2003) found an increase in the overall crystallinity of *Pinus pinaster* wood after SE treatment. This is consistent with results studied by Yamashiki *et al.* (1990), which shows that SE treatment causes an increase in crystallinity because cellulose molecules in amorphous zones become regularly arranged and form new crystalline regions. Thermal properties, especially thermal stability and thermal transitions of the amorphous components of wood play an important role in the production of fiber boards (Yang *et al.* 2007), briquettes, fuel pellets, and wood plastic composites (Salvadó *et al.* 2003; Stelte *et al.* 2011).

Although batch-type SE technology has been widely used, it has low production capacity, which causes a need for an additional steam generator, ultimately increasing production costs. Therefore, researchers have developed equipment for continuous steam explosion (CSE) (Chen *et al*. 2014; Feng *et al*. 2014). Tests have shown that the CSE equipment has a higher production capacity than SE and does not require an additional steam generator, resulting in less energy consumed, and it can be used with various types of materials; therefore, it is suitable for industrial production. They prepared modified plant fibers with a high aspect ratio using the CSE equipment and found that reinforcement of polyethylene and polypropylene with these modified fibers improved the general mechanical properties of the polymers (Chen *et al*. 2014; Feng *et al*. 2014).

The fact that various CSE treatment intensities are needed for different plant materials and applications means that it is important to investigate the effects of CSE on the composition, microstructure, and properties of plant fibers to facilitate the exploitation of plant biomass, improve efficiency, and reduce costs. In this study, eucalyptus (*Eucalyptus citriodora* Hook) wood (EW) was repeatedly subjected to CSE, using the previously designed CSE equipment. The surface composition, morphology, thermal properties, and crystal properties of the continuous steam exploded eucalyptus fibers (CSEEFs) were assessed. An understanding of the changes that occur in CSE-treated plant fibers is important for improving fiber modification and developing new applications of CSE technology.

EXPERIMENTAL

Materials and Preparation of CSEEFs

The EW used in this study was obtained from Guangdong Dingfeng Paper Co., Ltd. (Zhaoqing city, Guangdong province, China). The moisture content of the EW was 15 wt.%. EW was smashed with a crusher (WSG-Y250, Wensui Plastic Machinery Co., Ltd., Guangzhou, China) and screened through a sieve with a 12-mm-diameter mesh. A moisture analyzer (MB25, Ohaus Instruments Co., Ltd., Shanghai, China) was used to measure the moisture content of materials. Tap water (pH = 7.5, general hardness = 7) was added to the crushed EW to achieve a moisture content of 50 wt.%, and the wet EW was kept in sealed plastic bags for 24 h at room temperature. Then, the EW was continuously steam exploded nine times repeatedly (generating CSEEF-1 to CSEEF-9) using laboratory-designed CSE equipment.

The major parts of CSE equipment are screw, barrel, die, motor drive unit, and feeding device. The materials with 50 wt.% moisture content were continuously fed into the barrel. They were conveyed forward, compacted, and heated gradually under the action of high-speed rotation screw. The compression, shear, and friction among materials, the screw, and the internal walls of the barrel provide heat to materials. When the materials were conveyed to the die, the pressure and temperature of materials reached about 1 to 1.5 MPa and 120 to 150 °C, respectively. Then the compacted and heated wet materials were discharged continuously and rapidly from the 1 mm wide ring slit die. The high temperature and high pressure water in the particles vaporized and did work through expansion, thus destroying the dense and complicated micro-nanostructures of plant fiber bundles and obtaining CSE fiber. The CSE process takes about 8 seconds for particles from charging to the discharging. The moisture content of materials was adjusted to 50 wt.% after each round of CSE to replace moisture that had evaporated during treatment. The materials was stirred evenly and then measured moisture content three time after each round. The amount of water needed to adjust moisture content to 50 wt.% was calculated by the average moisture content of materials. Then, the materials was sprayed needed water and stirred evenly. Samples of EW and CSEEFs were obtained by random sampling and dried in an oven at 105 °C for 12 h for further analysis.

Methods

Chemical composition analysis

The chemical composition of EW and CSEEFs was analyzed using the standard National Renewable Energy Laboratory method (Sluiter *et al*. 2008). Samples were oven-dried at 105 °C, weighed to obtain oven-dry weight, and then extracted with ethanol prior to acid hydrolysis. The standard method uses a two-step acid hydrolysis. Then, high-performance liquid chromatography (Prominence LC-20A, Shimadzu, Japan) was used to determine the cellulose and hemicellulose contents in the hydrolysis liquid. Next, the lignin was fractionated into acid-insoluble and acid-soluble materials. Results were calculated on an oven-dry weight basis. Three repeated measurements were made for each sample to confirm the reproducibility of results.

Scanning electron microscopy (SEM)

Images of the surface morphology of EW and CSEEFs were obtained using a scanning electron microscope (model S-3700, Hitachi, Japan) operated in secondary electron mode with a beam current of 100 mA and an accelerating voltage of 20 kV. Samples were coated with a thin layer of gold using a vacuum coater (Leica EM ACE200, Leica Microsystems, Germany) before SEM analysis.

X-ray photoelectron spectroscopy (XPS)

Surface analysis of EW and CSEEFs was performed using an XPS instrument (AXIS Ultra DLD, Shimadzu Corporation, Japan) equipped with a monochromatic Al Kα X-ray source (15 kV, 5 mA) operated at 150 W and with an electron flood gun for charge compensation. Because the objective was to study the influence of CSE on the surface composition of fibers, samples were not extracted before analysis. Samples were formed into small sheets with diameters of 20 mm and thicknesses of 1 mm. Measurements were taken at two different locations on the surface of each sheet; at each location, the analyzed area was 300 μm × 700 μm. Low-resolution survey scans were taken with a 1-eV step and 160-eV pass energy, while high-resolution spectra were taken with a 0.1-eV step and 40-

eV pass energy. The oxygen to carbon atomic ratio (O/C) was determined from low-resolution spectra, and the relative amounts of differently bound carbons were determined from high-resolution C1s spectra. The relative sensitivity factors of carbon and oxygen are 0.278 and 0.780, respectively. The collected data were analyzed using CASA XPS version 2.3 (Casa Software Ltd., UK).

Differential scanning calorimetry (DSC)

Glass transition temperatures were determined with a differential scanning calorimeter (DSC 204 F1 Phoenix, Netzsch, Germany) in a nitrogen atmosphere. Samples (3 to 5 mg) were heated from 10 to 120 °C at a rate of 10 °C/min and held at 120 °C for 3 min to remove moisture, then cooled to -50 °C at a rate of 10 °C/min and held at -50 °C for 3 min. Samples were then heated from -50 to 250 °C at the same rate for the second scan. The glass transition temperature (T_g) was determined from the second scan. The T_g was taken as the midpoint of the change in heat capacity.

X-ray diffraction (XRD)

X-ray diffractograms of EW and CSEEFs were obtained with a Bruker D8 ADVANCE (Bruker, Germany) diffractometer (40 kV, 40 mA) by the refraction method using nickel-filtered Cu Kα radiation (λ = 1.54 Å). Scans were performed from 5° to 60° with increments of 0.04° and 0.2 s per step. Crystallinity was determined using the powder XRD method. The collected data were analyzed using MDI Jade (Materials Data Incorporated, US). The crystallization peaks and amorphous peaks were obtained by means of XRD-peak-differentiation-imitating analysis with same parameters for all samples, and the fitness error was about 6%.

Thermogravimetric analysis (TGA)

The thermal stability of EW and CSEEFs was studied using a TG209 F3 thermogravimetric analyzer (Netzsch, Germany). Approximately 10 mg of sample was heated from 25 to 700 °C at a rate of 10 °C/min. Nitrogen gas at a flow rate of 50 mL/min was used to protect samples from oxidation.

RESULTS AND DISCUSSION

Effect of CSE on the Chemical Composition of EW and CSEEFs

The calculated contents of the main components of EW and CSEEFs are shown in Table 1. The changes in chemical composition were primarily due to the loss of lignin and hemicellulose.

The lignin contents shown in Table 1 are the sum of acid-insoluble and acid-soluble lignin. As the CSE treatment time increased, the lignin content of CSEEFs decreased, although the downward trend gradually weakened. CSEEF-9 showed the greatest reduction of lignin content (32.4% compared with EW). The loss of lignin was due to the removal of fragments of degraded lignin during ethanol extraction; as the CSE treatment time increased, so did the accessibility, hence the removal of lignin degradation products.

The hemicellulose content decreased gradually as the CSE treatment time increased. Hemicellulose contents of CSEEF-9 have decreased 26.0% compared to EW. This is because a portion of hemicellulose is bound in a lignin-carbohydrate complex; thus, some of the hemicellulose was removed with lignin fragments during ethanol extraction.

Table 1. Relative Amounts of the Major Components of EW and CSEEFs

Samples	Lignin (%)	Hemicellulose (%)	Cellulose (%)
EW	27.26±0.58	20.58±0.96	51.88±0.46
CSEEF-1	26.11±0.45	17.44±0.60	49.95±0.65
CSEEF-2	25.22±0.61	15.50±1.33	46.77±1.37
CSEEF-3	23.77±0.59	15.21±0.69	47.79±1.25
CSEEF-4	22.73±0.67	16.16±1.13	46.80±1.06
CSEEF-5	20.78±0.49	15.26±1.27	48.78±0.41
CSEEF-6	20.54±0.81	17.89±1.32	50.39±0.80
CSEEF-7	19.19±0.63	17.85±0.44	51.46±1.45
CSEEF-8	19.03±0.49	17.03±0.51	49.63±0.75
CSEEF-9	18.44±0.47	15.24±0.57	50.01±0.94

CSE treatment had less of an effect on cellulose content. The cellulose content ranged between 46.80% and 51.88%. Possible reasons for this fluctuation include sample heterogeneity and analytical errors.

In fact, the content of three major components of samples remained about the same after CSE treatment. CSEEFs are known to have more ethanol extractive than EW, and this indirectly reflects the effect of CSE on the separation and degradation of EW composition. The separation and redistribution of composition changed the surface of fibers.

Effect of CSE on the Morphology of EW and CSEEFs

Scanning electron microscopy was used to examine the samples to determine the effect of CSE on the microstructure of the materials. Low-magnification SEM micrographs (×40) of EW and CSEEFs are shown in Fig. 2. The fiber cells of EW were regularly arranged and closely bound together into stiff bundles (Fig. 2a). The CSE treatments destroyed the structure of the fiber bundles; the bundles softened and curled, and the closely bonded fibers gradually separated. The degree of separation of fibers was related to the CSE treatment time (intensity). After one round of CSE (CSEEF-1), the size of the fiber bundles was reduced, but only a small number of fiber cells were stripped from the bundles (Fig. 2b). After four rounds (CSEEF-4), the fibers were almost completely separated from each other (Fig. 2e). However, after six CSE treatments, the separated fibers began to cluster together. This is probably because hemicellulose, lignin, and their degradation products adhered to the surface of fibers and "glued" the fibers together under the squeezing action of the screw of the CSE equipment.

Changes in fiber microstructure can be seen in the high-magnification SEM micrographs (×5000) shown in Fig. 3. The untreated EW fiber cells were rigid and tightly bound to adjacent fiber cells. Flaky material covered the cells, forming a relatively smooth surface (Fig. 3a). The surface of fibers was slightly fractured after one CSE treatment and severely damaged after three rounds of treatment. In CSEEF-3, attachments related to the middle lamella and primary wall were partially stripped, and some remnants on the surface formed local enrichment features (Fig. 3d).

As the CSE treatment time increased, the degree to which these attachments were stripped also increased. Microfibrils are clearly visible in the images of fibers from CSEEF-5 to CSEEF-9 (Fig. 3f to 4j); the microfibril angles shown in these images are about 20°. This indicates that the middle lamella, primary wall, and outermost layer of the secondary wall (S1) were almost completely removed after five CSE treatments, exposing the S2 layer (Fig. 1).

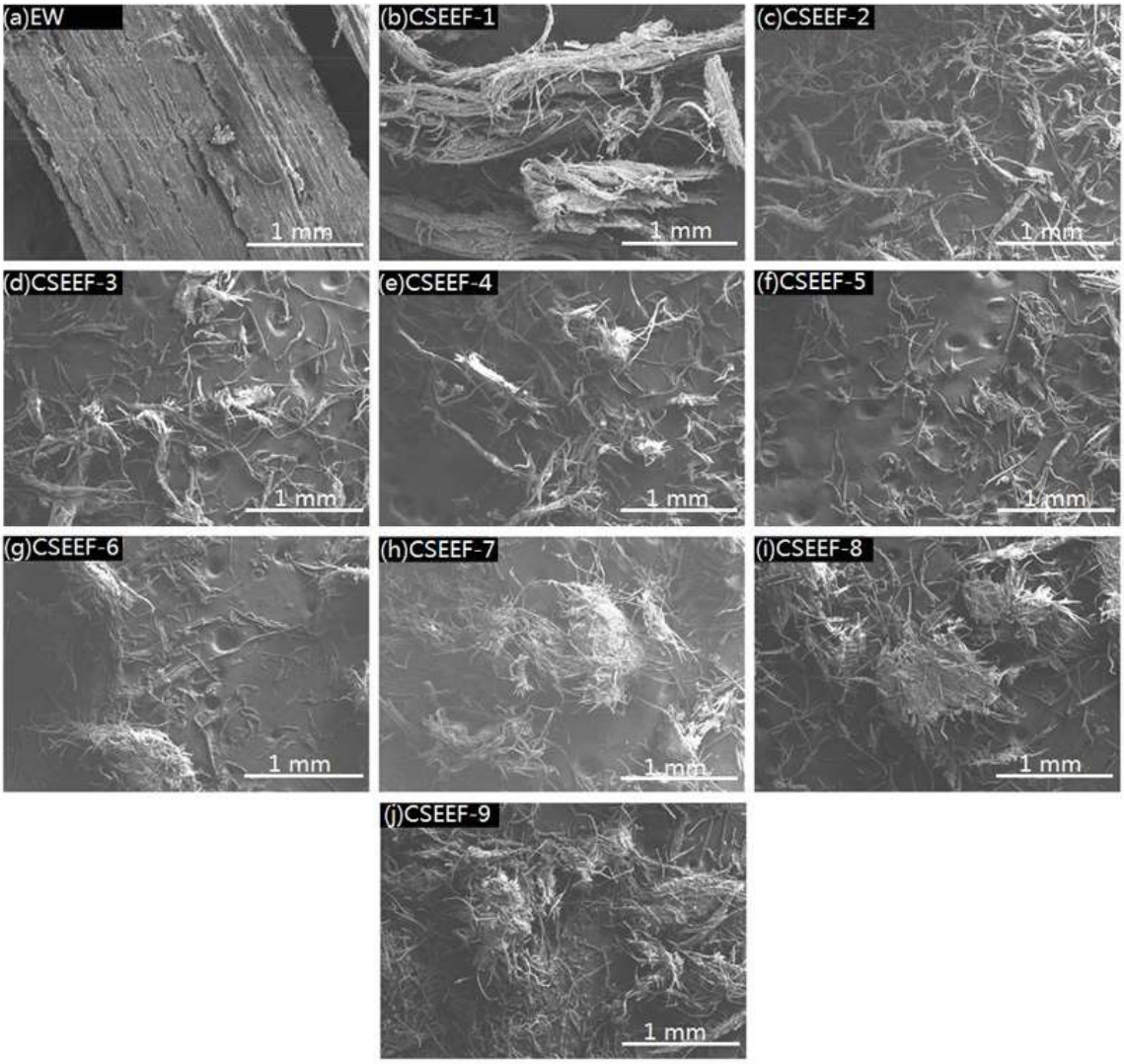

Fig. 2. SEM micrographs of EW and CSEEFs (×40)

Effect of CSE on the Surface Composition of Samples

XPS has long been used to assess the surface composition of plant fibers. The elemental composition of a layer *ca.* 10 nm thick at the sample surface is evaluated based on the C and O peak sizes and shapes. The carbon in cellulose, hemicellulose, lignin, and extractives can be categorized into four groups: C1 (C–C), C2 (C–O), C3 (O–C–O, C=O), and C4 (O=C–O). The chemical shifts relative to C1 (284.6 eV) for C2, C3, and C4 are 1.7 ± 0.1 eV, 3.1 ± 0.1 eV, and 4.4 ± 0.2 eV, respectively. In plant fibers, C1 exists in lignin, as well as in extractives, which are low-molecular weight compounds such as resin acids, triglycerides, fatty acids, and phenolics. C2 and C3 are found in the cellulose and hemicellulose, and C4 exists in carboxylic acids. The relative amounts of C1, C2, and C3 in lignin are 49%, 49%, and 2%, respectively. The C1 content in extractives is very high. The relative amounts of C2 and C3 in cellulose are 83% and 17%, respectively. The O/C atomic ratios were estimated from the carbon and oxygen peak intensities. The theoretical O/C atomic ratios of cellulose, lignin, and extractives are 0.83, 0.33, and 0.10, respectively. The fractions of the four classes of carbon atoms (C1/C1s, C2/C1s, C3/C1s, and C4/C1s) are equal to their contributions to the peak area (Dorris and Gray 1978a,b; Gray 1978).

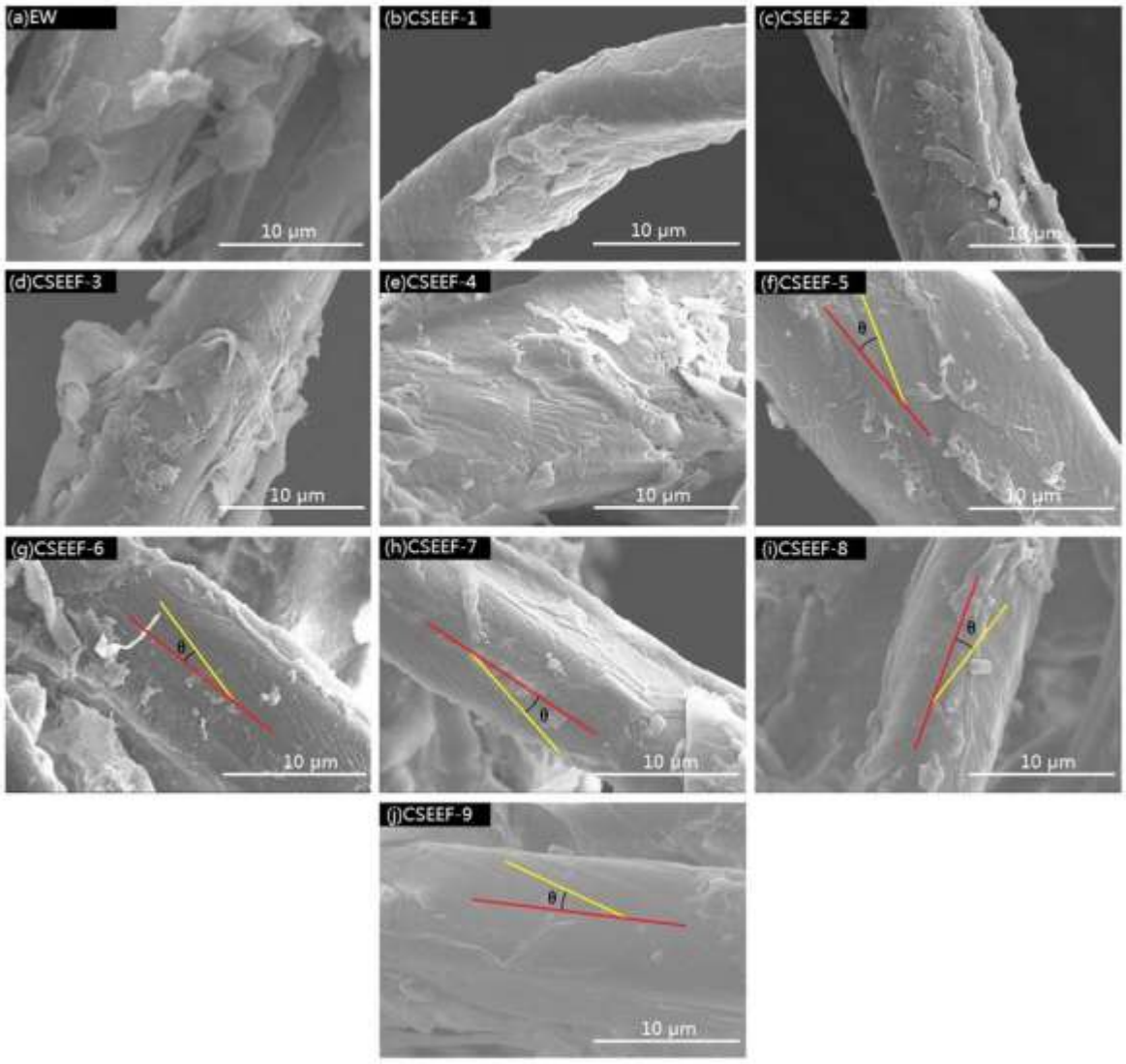

Fig. 3. SEM micrographs of EW and CSEEFs (×5000)

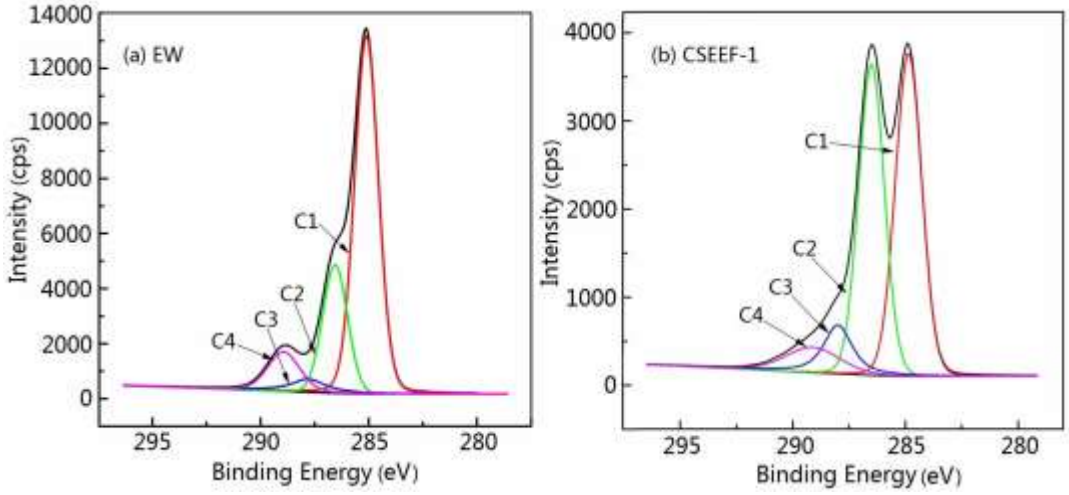

Fig. 4. C1s spectra of EW and CSEEF-1

Table 2. XPS Analysis of EW and CSEEFs

Samples	C_{1S}=100%				O/C
	C1 (%)	C2 (%)	C3 (%)	C4 (%)	
EW	62.85	22.59	4.78	9.78	0.37
CSEEF-1	43.12	40.33	9.16	7.39	0.41
CSEEF-2	45.34	38.93	6.88	8.85	0.43
CSEEF-3	45.76	37.07	7.93	9.24	0.45
CSEEF-4	42.84	39.96	8.82	8.38	0.46
CSEEF-5	39.37	43.94	9.24	7.45	0.49
CSEEF-6	35.71	43.13	11.74	9.42	0.50
CSEEF-7	35.96	46.62	9.67	7.75	0.53
CSEEF-8	32.56	46.52	11.85	9.07	0.55
CSEEF-9	29.42	44.62	16.82	9.14	0.57

The C1s spectra for EW and CSEEF-1 are shown in Fig. 4. The relative amounts of C1–C4 and the O/C atomic ratios for EW and CSEEFs are summarized in Table 2. The C1 content of EW was higher than that of CSEEF-1 (Fig. 4), which may be due to the high concentration of extractives in the exposed middle lamella of the EW fiber bundles. In addition to the decrease in the relative peak area of C1 in the CSEEF-1 spectrum compared with the EW spectrum, there were substantial increases in the relative peak areas of C2 and C3. These differences indicate that polysaccharides (cellulose and hemicellulose) constituted a larger proportion of the surface layer in CSEEF-1 than in EW. Thus, the O/C atomic ratio of CSEEF-1 was higher than that of EW. As the number of rounds of CSE treatment increased from 1 to 9, the relative amount of C1 decreased, while the C2 and C3 contents and the O/C atomic ratio increased. These trends indicate that the amounts of lignin and extractives attached to the surface of CSEEFs decreased with increasing CSE treatment time. The CSE treatments gradually damaged the compound middle lamella and S1 layer, exposing the cellulose microfibrils. CSEEF-9 had the greatest proportion of polysaccharides on the surface (the highest O/C atomic ratio). Overall, these results are consistent with the SEM results.

Changes in the Glass Transition Temperature of Lignin after CSE Treatment

A better understanding of the thermal transitions of the amorphous components of wood fiber will help in process design for the products manufacturing and also help to improve properties. The DSC curves and T_g values of the samples are shown in Fig. 5. The lignin of EW is composed primarily of coniferyl and sinapyl alcohol units along with a small amount of p-coumaryl alcohol. The T_g of EW was high because of the steric hindrance from the large coniferyl and sinapyl alcohol units.

As shown in Fig. 5, there was a broad endothermic transition at 170 to 200 °C for EW, while there were two endothermic transitions, at 50 to 130 °C and 130 to 190 °C, for the CSEEFs. The T_gs of the CSEEFs first decreased and then increased with increasing CSE treatment time, but the T_gs of CSEEF-9 were still lower than the T_g of EW.

Three factors contributed to these changes: 1) CSE disrupted the compact structure of the fiber cells, and the resulting degradation of hemicellulose and lignin reduced the number of chemical bonds between these components, thus reducing steric hindrance. This led to an increase in the molecular chain motion of lignin, allowing the glass transition to occur at a lower temperature (Bouajila *et al*. 2006). 2) There was a direct relationship between T_g and molecular weight. Degraded lignin has a lower molecular weight and,

therefore, a lower T_g. 3) Studies have shown that lignin depolymerization and repolymerization occur simultaneously during SE treatment (Li *et al*. 2007). Repolymerization of lignin fragments produces new high-molecular weight products with higher T_g. Lignin depolymerization during the first six CSE treatments lowered the T_g, while repolymerization of lignin during subsequent CSE treatments gradually raised the T_g.

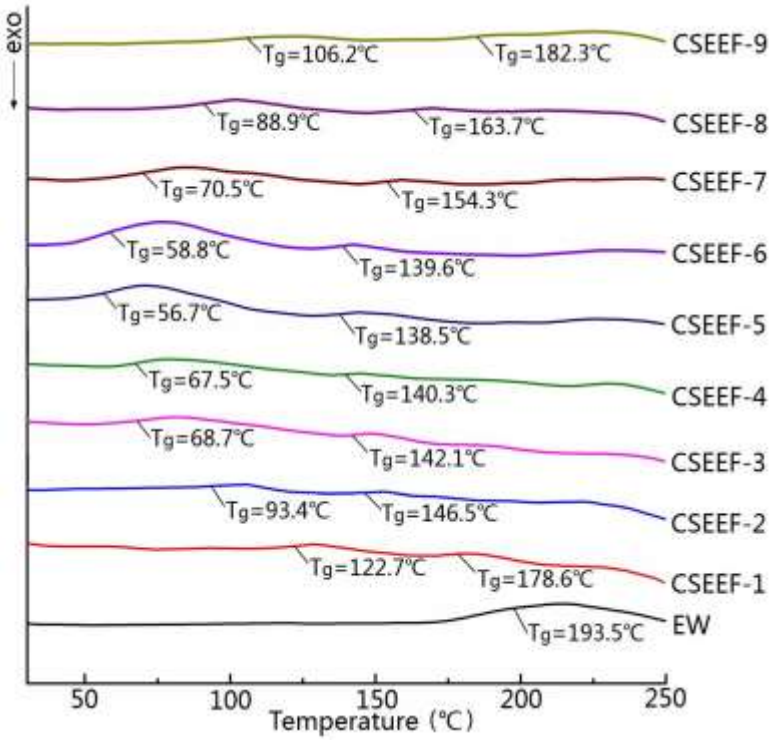

Fig. 5. DSC curves of EW and CSEEFs

Effect of CSE on the Crystallinity of Cellulose

Cellulose is partially crystallized. The XRD patterns of EW and CSEEFs (Fig. 6) showed diffraction peaks at 2θ = 16.6°, 22.7°, and 34.6°. These peaks indicate that the samples contained native lignocellulose, which includes both crystalline and amorphous cellulose. The allomorph of cellulose found in EW, cellulose I, was not converted to other allomorphs (cellulose II, III, and IV) by CSE treatment.

The crystallinity of EW and CSEEFs, as determined by XRD spectroscopy, is shown in Table 3. The crystallinity of samples decreased with increasing CSE treatment time. The CSE treatments broke the lignin seal and increased the specific surface area of the fibers, which increased the accessibility of cellulose. Part of the crystalline structure of cellulose was disrupted, so the crystallinity decreased. However, smaller decreases in the crystallinity of CSEEFs were observed after two CSE treatments, indicating that additional CSE treatments had a limited impact on the cellulose in fibers. Therefore, the strength of fibers can be maintained even with multiple CSE treatments, which is of great significance for the preparation of continuous steam exploded fibers for papermaking, reinforcement, and other similar applications.

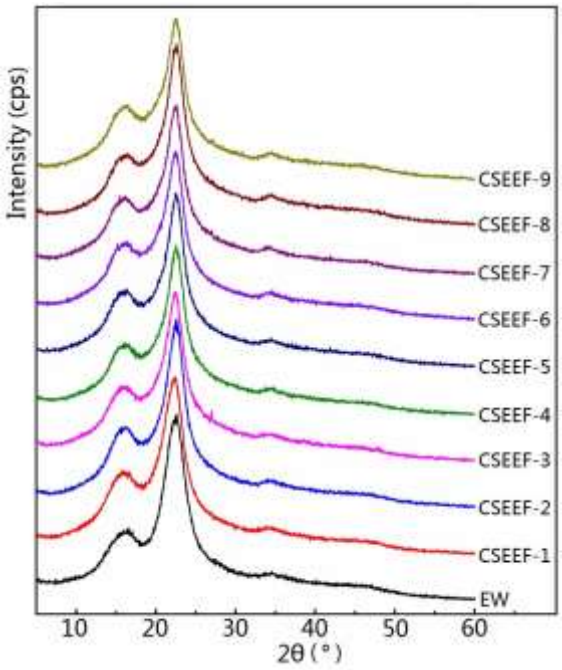

Fig. 6. XRD curves of EW and CSEEFs

Table 3. Crystallinity of EW and CSEEFs, as Determined by XRD

Samples	Crystallinity of samples (%)
EW	44.9
CSEEF-1	40.6
CSEEF-2	37.1
CSEEF-3	37.8
CSEEF-4	37.1
CSEEF-5	38.5
CSEEF-6	39.2
CSEEF-7	39.5
CSEEF-8	38.1
CSEEF-9	37.8

Effect of CSE on the Thermal Stability of EW

Thermal stability affects the use and processing of materials. Materials with different chemical compositions present different thermal behaviors. Derivative thermogravimetric curves of EW and CSEEFs are shown in Fig. 7. The thermal degradation of EW and CSEEFs can be divided into an evaporation stage (30 to 150 °C), a thermal pyrolysis stage (200 to 500 °C), and a thermal polycondensation stage (500 to 700 °C). The thermal pyrolysis stage is the main stage of thermal degradation of EW and CSEEFs. Pyrolysis of hemicellulose, a small amount of cellulose, and lignin occurred at 200 to 330 °C. The weight loss that took place between 330 and 500 °C is attributed to bulk pyrolysis of cellulose and lignin, and the corresponding peak temperature (the temperature at which the weight loss rate was maximized) was approximately 370 °C.

As shown in Fig. 7, the peak temperature of pyrolysis of the samples first increased and then decreased slightly as the CSE treatment time increased. CSEEF-6 had the greatest thermal stability. The reasons for this are as follows: on the one hand, CSE treatment reduced the percentage of hemicellulose that was easily degradable, which improved the thermal stability of the sample; on the other hand, CSEEFs have a larger specific surface

area and a lower crystallinity, which reduces the thermal stability of fibers. The first reason played a dominant role during the first six CSE treatments, while the latter reason was more important after the sixth treatment.

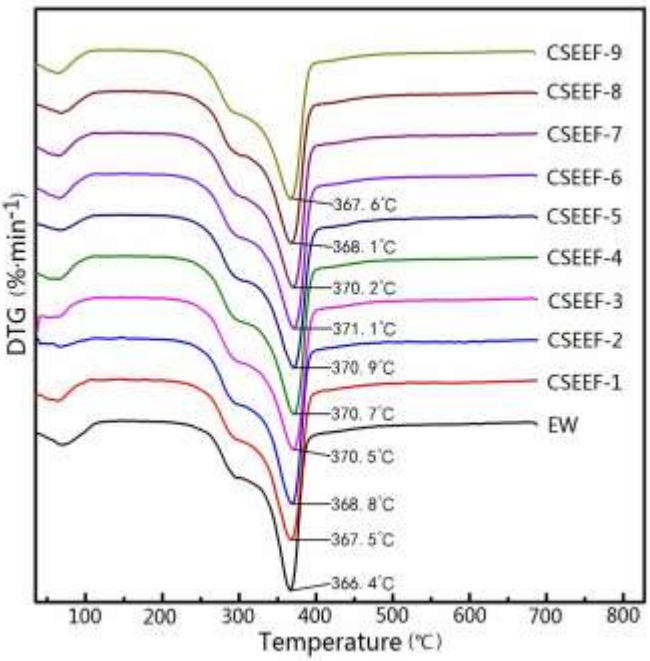

Fig. 7. Derivative thermogravimetric curves of EW and CSEEFs

CONCLUSIONS

1. The middle lamella, primary wall, and outermost layer of the secondary wall (S1) were progressively stripped from the surface with increasing treatment time of continuous steam explosion (CSE). The S2 layer was exposed after five treatments.
2. Eucalyptus fibers that had been treated by continuous steam explosion (CSEEFs) had more ethanol extractive than the untreated eucalyptus wood (EW), which indirectly reflects the effect of CSE treatment on the separation of EW compositions. The separation and redistribution of composition changed the surface of fibers.
3. The concentrations of extractives and lignin were highest on the surface of EW, and the exposed carbohydrate fraction gradually increased with increasing CSE treatment time. The O/C atomic ratios increased from 0.37 of EW to 0.57 of CSEEF-9.
4. EW exhibited a single glass transition near 193.5 °C, while CSEEFs had two glass transitions at lower temperatures. The T_gs of the CSEEFs decreased with each of the first five CSE treatments and then gradually increased. CSEEF-5 displayed the lowest T_gs (56.7 and 138.5 °C). The cellulose crystallinity of samples decreased with increasing CSE treatment time.
5. This study suggests that it is feasible to prepare fibers with different physical and chemical properties from different plant resources by changing the CSE treatment time, which will facilitate the use of plant fibers in various applications. For example, lowering the T_g of plant fibers broadens the thermal processing window; modification

of fiber surface properties will make it possible to improve bonding with different materials; and dissociation of fibers will help to improve the efficiency of fermentation or modification reactions.

6. An understanding of the effect of CSE treatment time on the properties of plant fibers will be helpful for improving the design of processes and equipment for fiber modification and for developing new applications of CSE technology.

ACKNOWLEDGMENTS

The authors acknowledge financial support from the National Natural Science Foundation of China (No. 51373058), the Science and Technology Planning Project of Guangdong Province, China (No. 2014B090921006), the Fundamental Research Funds for the Central Universities (No. 2015ZZ004), and the Specialized Research Fund for the Doctoral Program of Higher Education (No. 20120172130004).

REFERENCES CITED

Basurto Gutierrez, R., Escamilla Martinez, A., Moya Vega, S., Ramirez Rodriguez, E., and Becerra Becerra, J. (2012). "Chemical composition, digestibility and digestion kinetics of steam explosion-treated crop residues," *Rev. Mex. Cienc. Pecu.* 3(4), 407-425.

Bouajila, J., Dole, P., Joly, C., and Limare, A. (2006). "Some laws of a lignin plasticization," *J. Appl. Polym. Sci*. 102(2), 1445-1451. DOI: 10.1002/app.24299

Chen, F. Q., Liu, H. Y., Zhao, Y. Q., Feng, Y. H., Guo, R. B., Wu, Z. H., Chen, H. Z., Tang, H. L., and Qu, J. P. (2014). "*Caulis spatholobi* residue fiber reinforced biodegradable poly (propylene carbonate) composites: The effect of fiber content on mechanical and morphological properties," *Polym. Comp.* 35(2), 208-216. DOI: 10.1002/pc.22652

Chen, H. Z., and Liu, L. Y. (2007). "Unpolluted fractionation of wheat straw by steam explosion and ethanol extraction," *Bioresour. Technol.* 98(3), 666-676. DOI: 10.1016/j.biortech.2006.02.029

Dorris, G. M., and Gray, D. G. (1978a). "The surface analysis of paper and wood fibers by Esca-electron spectroscopy for chemical analysis - I. Applications to cellulose and lignin," *Cell. Chem. Technol.* 12(1), 9-23.

Dorris, G. M., and Gray, D. G. (1978b). "Surface analysis of paper and wood fibres by ESCA. II. Surface composition of mechanical pulps," *Cell. Chem. Technol.* 12(9), 721-734.

Feng, Y. H., Chen, H., Dong, X. L., Qu, J. P., He, H. Z., Xu, B. P., and Zhang, Y. Q. (2014). "Polyvinyl alcohol-modified *Pithecellobium clypearia* Benth herbal residue fiber/polypropylene composites," *Polym. Comp.* DOI: 10.1002/pc.23250

Gray, D. G. (1978). "Surface analysis of paper and wood fibres by ESCA. III. Interpretation of carbon (1s) peak shape," *Cell. Chem. Technol.* 12(9), 735-743.

Gray, D. G., Weller, M., Ulkem, N., and Lejeune, A. (2010). "Composition of lignocellulosic surfaces: Comments on the interpretation of XPS spectra," *Cellulose* 17(1), 117-124. DOI: 10.1007/s10570-009-9359-0

Hua, X., Kaliaguine, S., Kokta, B. V., and Adnot, A. (1993a). "Surface analysis of explosion pulps by ESCA Part 1. Carbon (1s) spectra and oxygen-to-carbon ratios," *Wood Sci. Technol.* 27(6), 449-459. DOI: 10.1007/BF00193868

Hua, X., Kaliaguine, S., Kokta, B. V., and Adnot, A. (1993b). "Surface analysis of explosion pulps by ESCA," *Wood Sci. Technol.* 28(1), 1-8. DOI: 10.1007/BF00193871

Kadla, J. F., and Gilbert, R. D. (2000). "Cellulose structure: A review," *Cellulose Chem. Technol.* 34(3-4), 197-216.

Koljonen, K., Stenius, P., and Buchert, J. (1997). "The surface chemistry of PGW pulp fibre fractions," *Proceedings of the International Mechanical Pulping Conference*, Stockholm, Sweden, pp. 407-411.

Law, K. N., and Bi, S. L. (1989). "Explosion pulping of black spruce," *TAPPI J.* 72(1), 111-114.

Law, K. N., and Valade, J. L. (1990). "The myth of fibre liberation during explosion pulping," *J. Pulp Pap. Sci.* 16(1), 41-42.

Li, J., Henriksson, G., and Gellerstedt, G. (2007). "Lignin depolymerization / repolymerization and its critical role for delignification of aspen wood by steam explosion," *Bioresour. Technol.* 98(16), 3061-3068. DOI: 10.1016/j.biortech.2006.10.018

Martín-Sampedro, R., Eugenio, M. E., García, J. C., Lopez, F., Villar, J. C., and Diaz, M. J. (2012). "Steam explosion and enzymatic pre-treatments as an approach to improve the enzymatic hydrolysis of *Eucalyptus globulus*," *Biomass Bioenerg.* 42, 97-106. DOI: 10.1016/j.biombioe.2012.03.032

Martín-Sampedro, R., Eugenio, M. E., Moreno, J. A., Revilla, E., and Villar, J. C. (2014). "Integration of a kraft pulping mill into a forest biorefinery: Pre-extraction of hemicellulose by steam explosion versus steam treatment," *Bioresour. Technol.* 153, 236-244. DOI: 10.1016/j.biortech.2013.11.088

Moniruzzaman, M. (1996). "Effect of steam explosion on the physicochemical properties and enzymatic saccharification of rice straw," *Appl. Biochem. Biotech.* 59(3), 283-297. DOI: 10.1007/BF02783570

Negro, M. J., Manzanares, P., Oliva, J. M., Ballesteros, I., and Ballesteros, M. (2003). "Changes in various physical/chemical parameters of Pinus pinaster wood after steam explosion pretreatment," *Biomass Bioenerg.* 25(3), 301-308. DOI: 10.1016/S0961-9534(03)00017-5

Salmén, L., and Ljunggren, S. (1996). "Physicochemical aspects of fiber processing," in: *The Chemistry and Processing of Wood and Plant Fibrous Material: Cellucon'94 Proceedings*, Kennedy, J. F., Phillips, G. O., and Williams, P. A. (eds.), Woodhead Publishing Limited, Abington Hall, UK, pp. 173-181. DOI: 10.1533/9781845698690

Samira, G., Emad, S., Salim, N. K., Hooman, Y., Ahmad, B., Mohammad, R. S., and Mohd, N. M. Z. (2015). "Basic effects of pulp refining on fiber properties—A review," *Carbohyd. Polym.* 115, 785-803. DOI: 10.1016/j.carbpol.2014.08.047

Salvadó, J., Velásquez, J. A., and Ferrando, F. (2003). "Binderless fiberboard from steam exploded *Miscanthus sinensis*: Optimization of pressing and pretreatment conditions," *Wood Sci. Technol*. 37, 279-286. DOI: 10.1007/s00226-003-0186-4

Sjöström, E. (1993). *Wood Chemistry: Fundamentals and Applications*, 2nd Ed., Academic Press, San Diego, CA.

Sluiter, A., Hames, B., Ruiz, R., Scarlata, C., Sluiter, J., Templeton, D., and Crocker, D. (2008). "Determination of structural carbohydrates and lignin in biomass,"

Laboratory Analytical Procedure (LAP), National Renewable Energy Laboratory, Golden, CO.

Stelte, W., Clemons, C., Holm, J. K., Ahrenfeldt, J., Henriksen, U. B., and Sanadi, A. R. (2011). "Thermal transitions of the amorphous polymers in wheat straw," *Ind. Crop. Prod.* 34, 1053-1056. DOI: 10.1016/j.indcrop.2011.03.014

Theuretzbacher, F., Lizasoain, J., Lefever, C., Saylor, M. K., Enguidanos, R., Weran, N., and Bauer, A. (2015). "Steam explosion pretreatment of wheat straw to improve methane yields: Investigation of the degradation kinetics of structural compounds during anaerobic digestion," *Bioresour. Technol.* 179, 299-305. DOI: 10.1016/j.biortech.2014.12.008

Wardrop, A. B. (1963). "Morphological factors involved in the pulping and beating wood fibres," *Svensk Papperstid.* 66(7), 231-247.

Yamashiki, T., Matsui, T., Saitoh, M., Okajima, K., Kamide, K., and Sawada, T. (1990). "Characterisation of cellulose treated by the steam explosion method. Part 1: Influence of cellulose resources on changes in morphology, degree of polymerisation, solubility and solid structure," *Brit. Polym. J.* 22(1), 73-83. DOI: 10.1002/pi.4980220111

Yang, H. P., Yan, R., Chen, H. P., Lee, D. H., and Zheng, C. G. (2007). "Characteristics of hemicellulose, cellulose and lignin pyrolysis," *Fuel*. 86, 1781-1788. DOI: 10.1016/j.fuel.2006.12.013

Zhang, Y. Z., and Chen, H. Z. (2012). "Multiscale modeling of biomass pretreatment for optimization of steam explosion conditions," *Chem. Eng. Sci.* 75, 177-182. DOI: 10.1016/j.ces.2012.02.052

Article submitted: September 17, 2015; Peer review completed: November 1, 2016; Revised version received and accepted: December 2, 2016; Published: December 17, 2015.
DOI: 10.15376/biores.11.1.1417-1431